

SCIENTIFIC REPORTS



OPEN

p38 α deficiency restrains liver regeneration after partial hepatectomy triggering oxidative stress and liver injury

Sergio Rius-Pérez¹, Ana M. Tormos¹, Salvador Pérez¹, Isabela Finamor¹, Patricia Rada^{2,3}, Ángela M. Valverde^{2,3}, Angel R. Nebreda^{4,5}, Juan Sastre¹ & Raquel Taléns-Visconti⁶

p38 α MAPK negatively regulates the G₁/S and G₂/M cell cycle transitions. However, liver-specific p38 α deficiency impairs cytokinesis and reduces hepatocyte proliferation during cirrhosis and aging in mice. In this work, we have studied how p38 α down-regulation affects hepatocyte proliferation after partial hepatectomy, focusing on mitotic progression, cytokinesis and oxidative stress. We found that p38 α deficiency triggered up-regulation of cyclins A1, B1, B2, and D1 under basal conditions and after hepatectomy. Moreover, p38 α -deficient hepatocytes showed enhanced binucleation and increased levels of phospho-histone H3 but impaired phosphorylation of MNK1 after hepatectomy. The recovery of liver mass was transiently delayed in mice with p38 α -deficient hepatocytes vs wild type mice. We also found that p38 α deficiency caused glutathione oxidation in the liver, increased plasma aminotransferases and lactate dehydrogenase activities, and decreased plasma protein levels after hepatectomy. Interestingly, p38 α silencing in isolated hepatocytes markedly decreased phospho-MNK1 levels, and silencing of either p38 α or Mnk1 enhanced binucleation of hepatocytes in culture. In conclusion, p38 α deficiency impairs mitotic progression in hepatocytes and restrains the recovery of liver mass after partial hepatectomy. Our results also indicate that p38 α regulates cytokinesis by activating MNK1 and redox modulation.

p38 α is a redox sensitive MAPK ubiquitously expressed at high levels in most cell types¹. It is also activated by environmental and genotoxic stress and plays key roles in the control of cell proliferation, differentiation and survival, as well as in the regulation of the inflammatory response²⁻⁴.

p38 α MAPK regulates the G₁/S and G₂/M cell cycle checkpoints prior to DNA synthesis and cell division, respectively⁵⁻⁷. Increased proliferation and impaired differentiation have been traditionally considered hallmarks of p38 α -deficient cells⁶. Thus, it was reported that mice with p38 α -deficient hepatocytes exhibited enhanced hepatocyte proliferation after partial hepatectomy (PHx)⁸ and developed more liver tumours with increased number of proliferative cells⁹. Accordingly, activation of p38 MAPK resulted in growth arrest and inhibition of DNA synthesis in cultured foetal rat hepatocytes³. In addition, inhibition of p38 MAPK *in vivo* was sufficient to trigger a marked increase in the number of proliferating hepatocytes⁵. However, paradoxically, we recently found that liver-specific p38 α deficiency lowered hepatocyte proliferation and enhanced hepatocyte binucleation due to cytokinesis failure in both biliary cirrhosis and aging^{3,10}.

Interestingly, hepatocytes are able to change from polyploid to diploid, and from binucleated to mononucleated with reduced ploidy by a phenomenon called somatic 'reductive mitoses', due to multipolar mitotic spindles¹¹. In fact, ploidy reversal is a useful tool to enhance hepatocyte proliferation¹². This prompted us to enquire how hepatocyte proliferation evolves when the brake exerted by p38 α in the G₁/S and G₂/M cell cycle transitions

¹Department of Physiology, University of Valencia. Burjassot, Valencia, 46100, Spain. ²Instituto de Investigaciones Biomédicas Alberto Sols (Centro Mixto CSIC-UAM), Arturo Duperier 4, 28029, Madrid, Spain. ³Centro de Investigación Biomédica en Red de Diabetes y Enfermedades Metabólicas Asociadas (CIBERdem), ISCIII, 28029, Madrid, Spain. ⁴Institute for Research in Biomedicine (IRB Barcelona), Barcelona Institute of Science and Technology, 08028, Barcelona, Spain. ⁵ICREA, Pg. Lluís Companys 23, 08010, Barcelona, Spain. ⁶Department of Pharmacy and Pharmaceutical Technology and Parasitology, University of Valencia. Burjassot, Valencia, 46100, Spain. Correspondence and requests for materials should be addressed to R.T.-V. (email: raquel.talens@uv.es)

is released. Thus, our aim was to study hepatocyte proliferation and liver regeneration after partial hepatectomy in mice with p38 α -deficient hepatocytes. We also determined whether p38 α deficiency leads to oxidative stress after partial hepatectomy.

Results

p38 α MAPK deficiency releases the brake with cyclins. p38 α is a negative regulator of cyclins, accordingly its deficiency triggered up-regulation of the mRNA of *Cyclins A1, B1, B2, and D1* under basal conditions and after partial hepatectomy, and also induced the expression of *Cdc25b* after PHx (Fig. 1A). The increase in *Cyclin B2* expression in the liver of p38 α knockout mice after hepatectomy was remarkable in comparison with wild type mice.

We also performed western blotting of cyclins D1 and B1, which shows that under basal conditions there were indeed increased levels of these cyclins upon p38 α deficiency (see Fig. 1B and Supplementary Fig. S1). However, after partial hepatectomy these levels did not further increase and maintained similar levels to those of wild type mice.

p38 α MAPK deficiency triggers cytokinesis failure after partial hepatectomy likely through reduced MNK1 phosphorylation. Immunohistochemistry of PCNA and phospho-H3 (p-H3) in livers of wild type and p38 α knockout mice showed a large increase in the mitotic index (calculated as p-H3/PCNA ratio) in p38 α knockout animals after PHx (Fig. 2A,B). Moreover we performed western blotting of nuclei isolated from whole livers to detect PCNA and p-H3. As expected, partial hepatectomy was associated with hepatocyte proliferation evidenced by increased PCNA protein levels, which occurred in both wild type and p38 α knockout livers (Fig. 2C and Supplementary Fig. S2A). Interestingly, a marked increase in p-H3 occurred only in p38 α deficient hepatocytes after PHx but not in wild type hepatocytes (Fig. 2C and Supplementary Fig. S2A). Besides, the lack of p38 α in hepatocytes caused an increase in p21 and p53 levels under basal conditions, but after partial hepatectomy these proteins were down-regulated (Fig. 2C and Supplementary Fig. S2A). Our previous findings indicated a failure to complete mitosis due to cytokinesis blockade as the cause of the high mitotic index in p38 α deficient hepatocytes^{3,10}. Hence, we measured phospho-MNK1 levels, as a critical p38 α downstream signaling mediator involved in centriolin localization during mitosis. We found that p38 α deficiency decreased phospho-MNK1 levels (Fig. 2D and Supplementary Fig. S2B). Furthermore, the analysis of MNK1 localization by immunofluorescence during the cell cycle revealed the co-localization of MNK1 and tubulin filaments during anaphase in sections from wild type livers, whereas MNK1 was not observed around tubulin filaments in p38 α knockout livers (Fig. 3).

p38 α MAPK deficiency triggered a transient delay in liver regeneration after partial hepatectomy. p38 α deficiency triggered a transient delay in liver regeneration after partial hepatectomy (Fig. 4A). Thus, at 72 h after partial hepatectomy wild type mice recovered the liver mass to a higher degree compared to p38 α knockout mice (Fig. 4A). However, at 1 week after hepatectomy the liver mass in p38 α knockout mice was completely recovered as in the control group.

This transient reduction in the recovery of the liver mass was associated with increased binucleation rates in p38 α deficient hepatocytes (binucleated hepatocytes/total hepatocytes) (Fig. 4B,C), in accordance with our previous results. However, we did not observe any difference in apoptosis between wild type and p38 α knockout livers (Fig. 4D). It is noteworthy that the decrease in binucleation after hepatectomy was observed in both wild type and p38 α knockout mice (Fig. 4C).

p38 α MAPK deficiency triggers oxidative stress and liver injury after partial hepatectomy. In livers of mice with p38 α -deficient hepatocytes, we observed that oxidized glutathione (GSSG) levels increased markedly at 72 h after partial hepatectomy (Fig. 5A). In addition, the lack of p38 α enhanced liver injury evidenced by the remarkable increase in plasma aminotransferases and lactate dehydrogenase activities found at 72 h after partial hepatectomy (Fig. 5B–D). Furthermore, a decrease in plasma protein levels – a sign of impaired liver function – was observed in mice with p38 α -deficient hepatocytes after PHx but not in wild type mice (Fig. 5E).

p38 α MAPK silencing in cultured hepatocytes increases binucleation through blockade of MNK1 phosphorylation. As MNK1 is an important mediator of p38 α signaling in the regulation of cytokinesis, we silenced both p38 α and Mnk1 in mouse primary hepatocytes (Fig. 6A and Supplementary Fig. S3A). Down-regulation of either p38 α or Mnk1 caused a clear increase in the binucleation of cultured hepatocytes (Fig. 6B). Importantly, p38 α silencing in primary hepatocytes resulted in a marked decrease in phospho-MNK1 levels, and we also observed the up-regulation of p21 (Fig. 6C and Supplementary Fig. S3B), consistent with the results in mice with p38 α -deficient hepatocytes.

Discussion

Binucleation has its pros and cons. It has some potential advantages, such as gain of function or genetic protection¹³. However it was considered a disadvantage when liver needs to grow^{14,15}. Binucleated hepatocytes seem to meet more difficulties when undergoing cell cycle as they have more complexity^{14,15}. This hypothesis has been questioned since Duncan and collaborators reported that hepatocytes are able to reverse its ploidy¹¹. Ploidy reversal has casted doubt upon classical hepatocyte proliferation principles that considered polyploid hepatocytes as a growing disadvantage. A remarkable feature of liver regeneration after partial hepatectomy in mice is the reduction in the percentage of binuclear polyploid hepatocytes and the increase in the percentage of mononuclear polyploid hepatocytes^{16–21}. During liver regeneration after 70% partial hepatectomy, diploid mononuclear, polyploid mononuclear, and polyploid binuclear hepatocytes all may enter the cell cycle leading generally to mononuclear

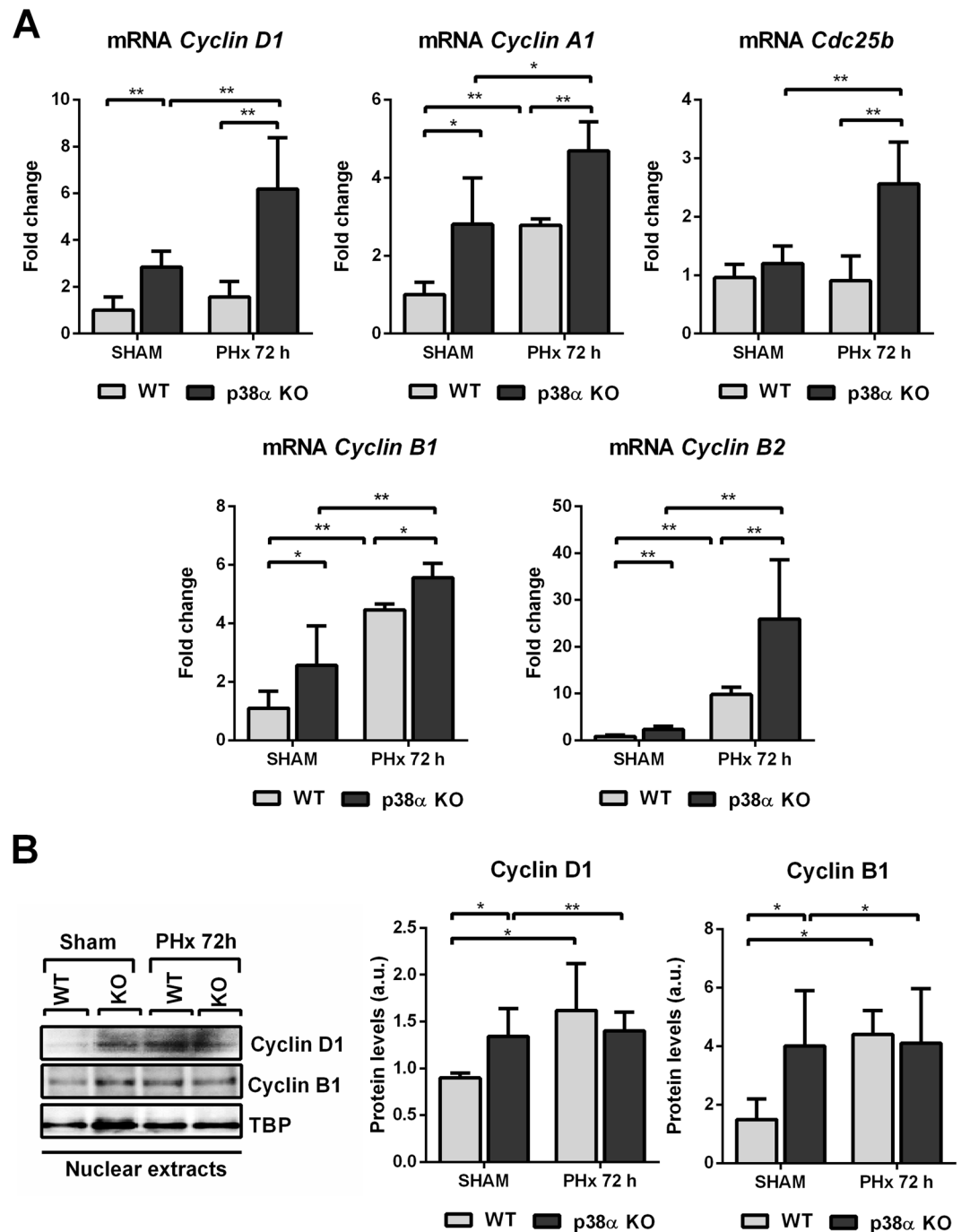


Figure 1. Effect of liver specific p38 α MAPK deficiency on cyclin mRNA expression after partial hepatectomy. **(A)** Real-time PCR analysis of the mRNA relative expression for *Cyclin D1*, *A1*, *Cdc25b*, *B1* and *B2* in liver 72 hours after hepatectomy (PHx). Data (mean and SD) are shown as fold increase in mRNA level compared to the control and were normalized by TATA-binding protein mRNA. **(B)** Representative western blot images and densitometries for cyclin D1 and cyclin B1 in nuclear extracts of livers from sham wild type and p38 α knockout mice and at 72 hours after PHx. TBP was used as a loading control. * $P < 0.05$; ** $P < 0.01$. WT, wild type mice; KO, p38 α knockout mice; PHx, partial hepatectomy.

daughter cells, a majority of them polyploid^{16–21}. At present it is unknown how highly binucleated hepatocytes face liver regeneration and whether p38 α MAPK plays a role in this regard.

Partial hepatectomy is a proliferative stimulus that induces compensatory growth in the liver and represents the most commonly intervention used for studying liver regeneration because it lacks massive necrosis or inflammation²². After 5 to 7 days of partial hepatectomy, rodents have usually recovered most of the original liver mass²³. Intense liver growth takes place on the first 6 days and many mitotic processes are completed by day 3²².

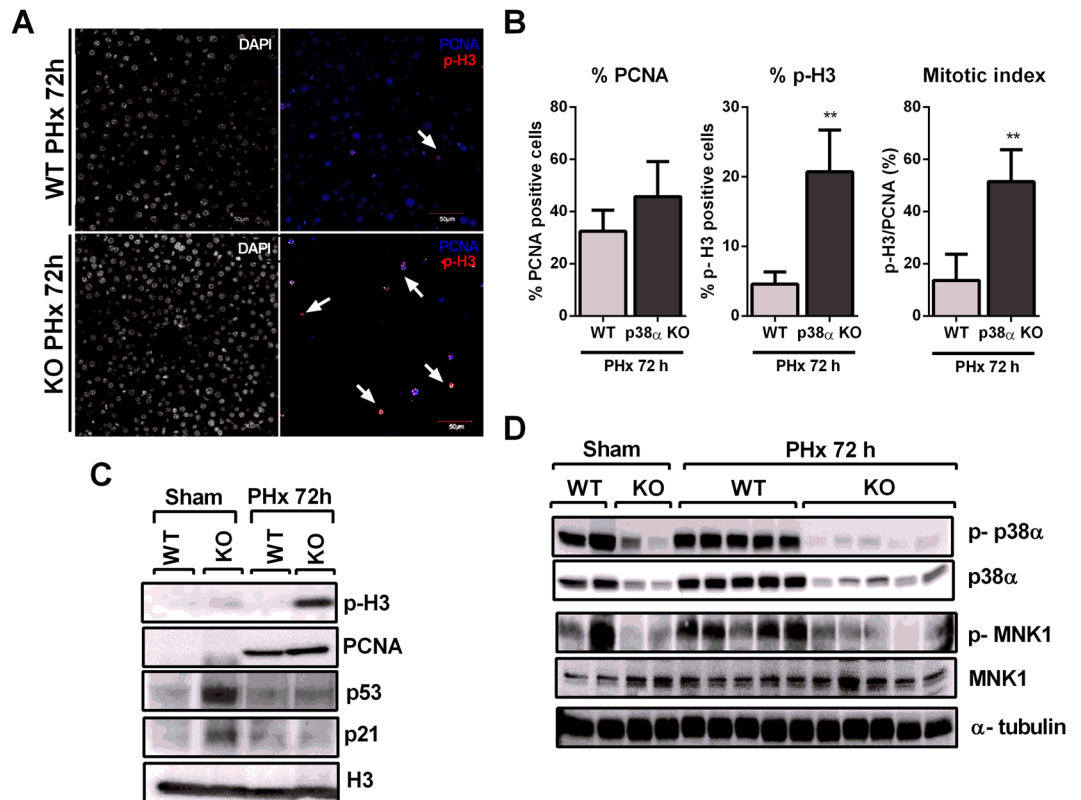


Figure 2. p38 α MAPK deficiency reduces MNK1 phosphorylation and triggers cytokinesis failure after partial hepatectomy. (A) Representative immunohistochemistry images of liver sections from wild type and liver specific p38 α knockout mice after partial hepatectomy. Red, phosphorylated histone 3 (p-H3); blue, PCNA; white, DAPI. A minimum of four experiments were performed for each group of animals. Scale bars = 50 μ m. (B) Quantification of the percentage of PCNA-positive cells, p-H3-positive cells, and mitotic index expressed as p-H3/PCNA ratio. Data are shown as mean and SD. ** $P < 0.01$. (C) Representative western blot images for p-H3, PCNA, p53, p21 and H3 in nuclear extracts of livers from sham wild type and p38 α knockout mice and at 72 hours after PHx. H3 was used as loading control. (D) Representative western blot for p-p38 α , p38 α , p-MNK1 and MNK1 from sham and after PHx livers of wild type and p38 α knockout mice. α -tubulin was used as loading control. WT wild type mice; KO p38 α knockout mice; PHx partial hepatectomy.

Our results show that binucleated p38 α -deficient hepatocytes were able to divide into mononuclear hepatocytes in order to efficiently proliferate. Hepatocytes deficient in p38 α MAPK from mice could reduce their binucleation rates when a compensatory hepatomegaly after liver resection is needed, although p38 α deficient hepatocytes were still more binucleated.

The liver ratio in mice with p38 α -deficient hepatocytes was significantly reduced at 3 days after partial hepatectomy compared to those from wild type mice, but at 1 week after hepatectomy the liver mass was completely recovered as in the control group. It has been reported that p38 α is rapidly inactivated at 30 min after partial hepatectomy and later on it is re-activated at 12 h after partial hepatectomy². In Supplementary Figs S4 and S5 we show that p38 α is re-activated at 24 h after hepatectomy but it is still less active than in controls, and Fig. 2 shows that it is completely reactivated at 72 h after hepatectomy. Hence, the re-activation of p38 α between 24 and 72 h after hepatectomy would be required for normal recovery of the liver mass during this period, whereas later on liver regeneration occurs independently from p38 α . Indeed, one week after partial hepatectomy p38 α phosphorylation is similar to controls and its deficiency does not affect significantly markers of hepatocyte mitosis and proliferation, which are similar to controls (see Supplementary Figs S4 and S5).

The lack of p38 α releases the brake on cyclins A1, B1, B2, and D1, but it could be again impairing the last stage of mitosis leading to cytokinesis failure. Accordingly, the high *cyclin A* and *cyclin B* mRNA levels may be due to mitotic arrest. Nevertheless, after hepatectomy it is likely that post-transcriptional regulatory mechanisms of the cell cycle control the protein levels of cyclins B1 and D1, which were similar in p38 α deficient mice and wild type mice.

After 72 hours of hepatectomy, p38 α knockout hepatocytes displayed higher nuclear levels of phosphorylated H3 in comparison with wild type hepatocytes. Thus, blockade of cytokinesis would trigger the accumulation of hepatocytes in the mitotic stage²⁴. In addition, under basal conditions, p38 α knockout hepatocytes show higher levels of p21 protein, which has been usually linked to the inhibition of cell cycle progression^{25–27}. It is intriguing that the release of one cell cycle brake, such as p38 α , results in the up-regulation of another brake, such as p21, which seems to be due to the high p53 levels associated with p38 α deficiency. Moreover, the mitogen stimulation

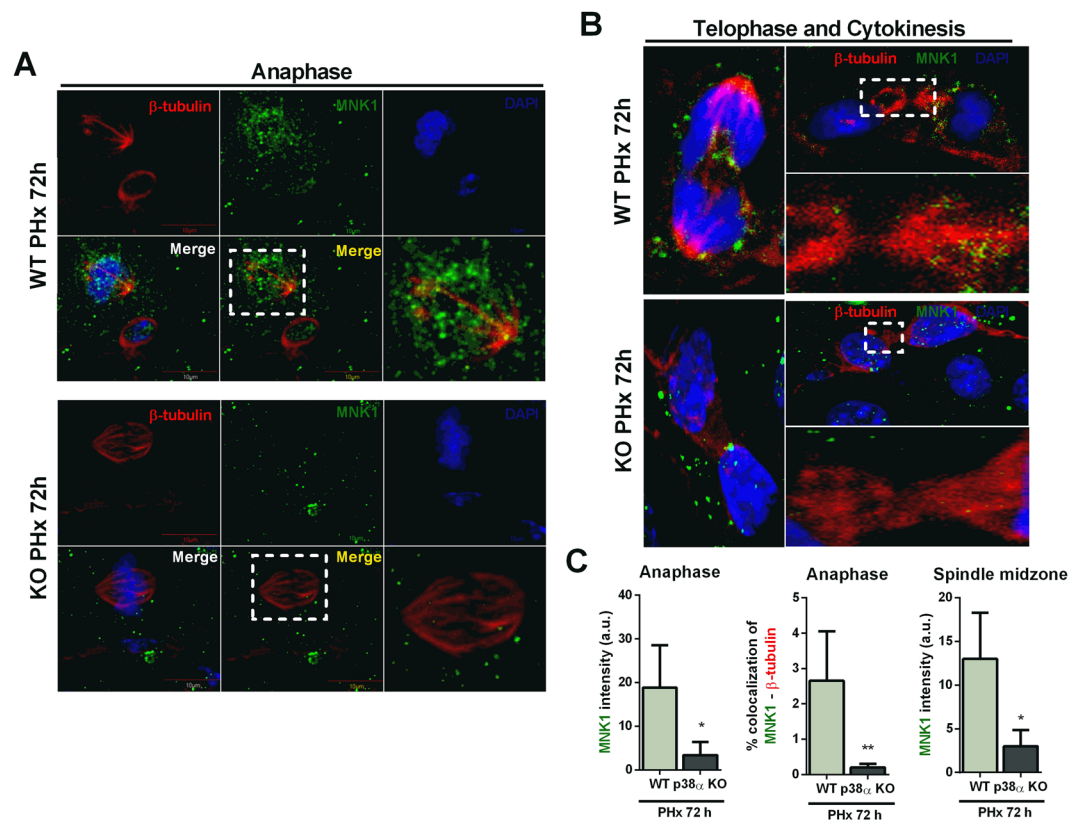


Figure 3. p38 α MAPK modulates MNK1 localization during the cell cycle after partial hepatectomy. (A) Representative immunohistochemistry images of hepatocytes in anaphase of wild type and p38 α knockout liver sections after partial hepatectomy. (B) Representative immunohistochemistry images of hepatocytes in telophase and cytokinesis of wild type and p38 α knock out liver sections after partial hepatectomy. Red, β -tubulin; green, MNK1; blue, DAPI. A minimum of four experiments were performed for each groups of animals. Scale bars = 10 μ m. (C) Fluorescence intensity of MNK1 staining and quantification of the colocalization of MNK1 and β -tubulin staining in immunohistochemistry images of hepatocytes in anaphase and fluorescence intensity of MNK1 in spindle midzone in cytokinesis images of wild type and p38 α knockout liver sections after partial hepatectomy. Data are shown as mean and SD. * $P < 0.05$; ** $P < 0.01$. WT, wild type mice; KO, p38 α knockout mice; PHx, partial hepatectomy.

associated with partial hepatectomy caused down-regulation of both p53 and p21 in the knockout mice. In fact, the decrease in p21 levels is likely to be due to the reduction of p53 levels upon hepatectomy.

Previous work has reported the requirement of p38 α for mitosis entry, proper spindle assembly and checkpoint functions in human, mouse, and rat-kangaroo cells²⁸ as well as HCT116 cells²⁴, and, in this regard, our results support a similar function for p38 α in hepatocytes *in vivo*.

Campbell and collaborators reported that p38 is rapidly inactivated 30 minutes after partial hepatectomy, corresponding with the activation of protein synthesis, and re-activated after 12 h, concluding that p38 α activity does not appear to be required for DNA replication *in vivo* during liver regeneration². In agreement with these findings, low p38 α MAPK activity was found during embryonic development⁵. Therefore, p38 α might not be required for DNA synthesis in hepatocytes, but it certainly regulates mitotic completion and cytokinesis.

Regarding the downstream pathways regulated by p38 α that could control cytokinesis, we show that p38 α clearly targets MNK1 in the liver. As described by Rannou and collaborators²⁹, dephosphorylation of MNK1 leads to the generation of multinucleated cells by deregulating centriolin localization and thus, affecting cytokinesis³⁰. In fact, the *Drosophila* Mnk1 orthologue (Lk6) interacts with microtubules and localizes to the centrosomes^{31,32} and it is necessary for cell abscission²⁹. We observed reduced MNK1 phosphorylation in p38 α -deficient hepatocytes both *in vivo* and in culture, and experiments with isolated hepatocytes demonstrate that MNK1 is responsible, at least in part, for the binucleation induced by p38 α deficiency.

In addition, the higher glutathione oxidation observed in p38 α -deficient livers after partial hepatectomy could also contribute to the cytokinesis blockade. We previously showed that oxidative stress induces hepatocyte binucleation during the isolation of hepatocytes³³. The same glutathione redox status was found in both wild type and p38 α -deficient livers under basal conditions, but p38 α knockout mice subjected to partial hepatectomy exhibited higher glutathione oxidation and consequently more oxidative stress in the liver. Therefore, the impact of oxidative stress on cytokinesis failure during the hepatectomy-induced proliferative response should be considered. Furthermore, although liver regeneration takes place in absence of p38 α , it is associated with oxidative stress, tissue injury, and impaired hepatic function.

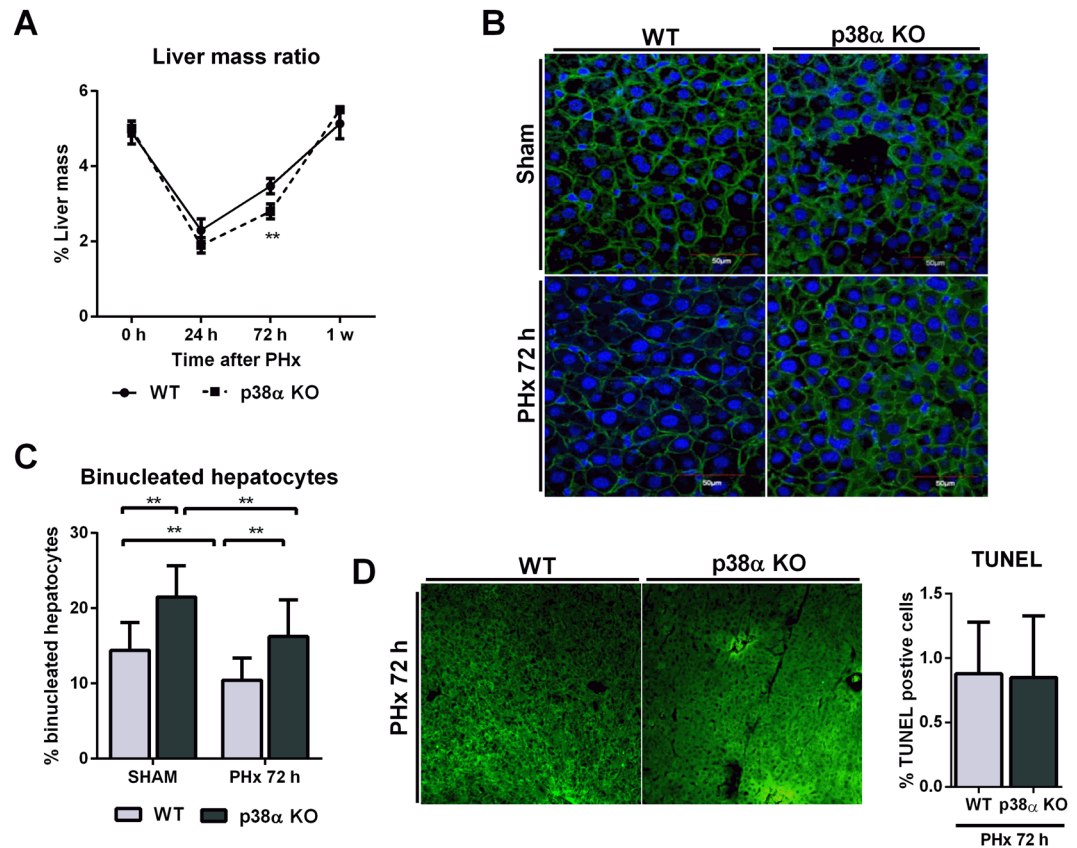


Figure 4. p38 α MAPK deficiency restrains liver regeneration after partial hepatectomy and induces hepatocyte binucleation. **(A)** Liver mass ratio, expressed as the ratio: liver weight/body weight (%), in sham wild type and p38 α knockout mice 24 h, 72 h and one week after partial hepatectomy. Data are shown as mean and SD. ****** $P < 0.01$. **(B)** Representative images of β -catenin (green) and DAPI (blue) immunohistochemistry in sham and 72 hours after PHx of wild type and p38 α knockout liver mice. Scale bars = 50 μ m. **(C)** Quantification of the binucleation rate (%) (binucleated hepatocytes / total hepatocytes) in sham and after 72 h of PHx based on the immunohistochemistry analysis. At least 20 fields per animal were examined. Data are shown as mean and SD. ****** $P < 0.01$. **(D)** Representative TUNEL immunohistochemistry images from wild type and p38 α knockout liver sections after PHx (scale bars = 50 μ m) and quantification of TUNEL-positive cells expressed as percentage of TUNEL-positive cells/total nuclei. A minimum of four experiments were performed for each group of animals. WT wild type mice; KO p38 α knockout mice; PHx partial hepatectomy.

In conclusion, our results suggest that p38 α is necessary for normal hepatocyte mitotic progression and contributes to cytokinesis by activating MNK1 and perhaps also by redox modulation. Its deficiency triggers a transient delay in the recovery of liver mass as well as oxidative stress, tissue injury, and impaired hepatic function after partial hepatectomy.

Methods

Animals. p38 α MAPK was specifically down-regulated in hepatocytes by using mice carrying p38 α floxed alleles and the Afp-Cre transgene that expresses Cre under the control of the α -fetoprotein promoter, which is active during embryonic hepatic development. The liver-specific p38 α knockout mice were kept in a C57BL/6 genetic background³⁴. We performed the partial hepatectomy experiments with wild type and p38 α MAPK knockout mice of 4 weeks-old. p38 α knockout mice exhibited some abnormalities in the actin cytoskeleton from 8–10 weeks of age as we previously reported¹⁰. Therefore, we preferred to assess liver regeneration in these mice just after weaning when their actin filaments were well conserved and only the deficiency in MNK1-phosphorylation was likely to affect the completion of cytokinesis in proliferating hepatocytes. Otherwise, the impairment in actin polymerization associated with p38 α deficiency that we described in our previous work could have a significant effect on cytokinesis and liver regeneration. For primary hepatocyte cell culture male C57BL/6 mice at 3–4 months of age were used. The *in vitro* experiments were performed in wild type mice at 8 weeks of age to selectively target MNK1 or p38 α for binucleation studies in mature livers avoiding the potential bias of mice livers still maturing and undergoing polyploidization at 4 weeks of age and more prone to proliferation upon hepatocyte isolation. Four to eight animals were used for each experimental group in all cases.

All mice received care in accordance with the criteria outlined in the Guide for the Care and Use of Laboratory Animals (NIH publication 86–23 revised 1985) and they were maintained under controlled conditions of

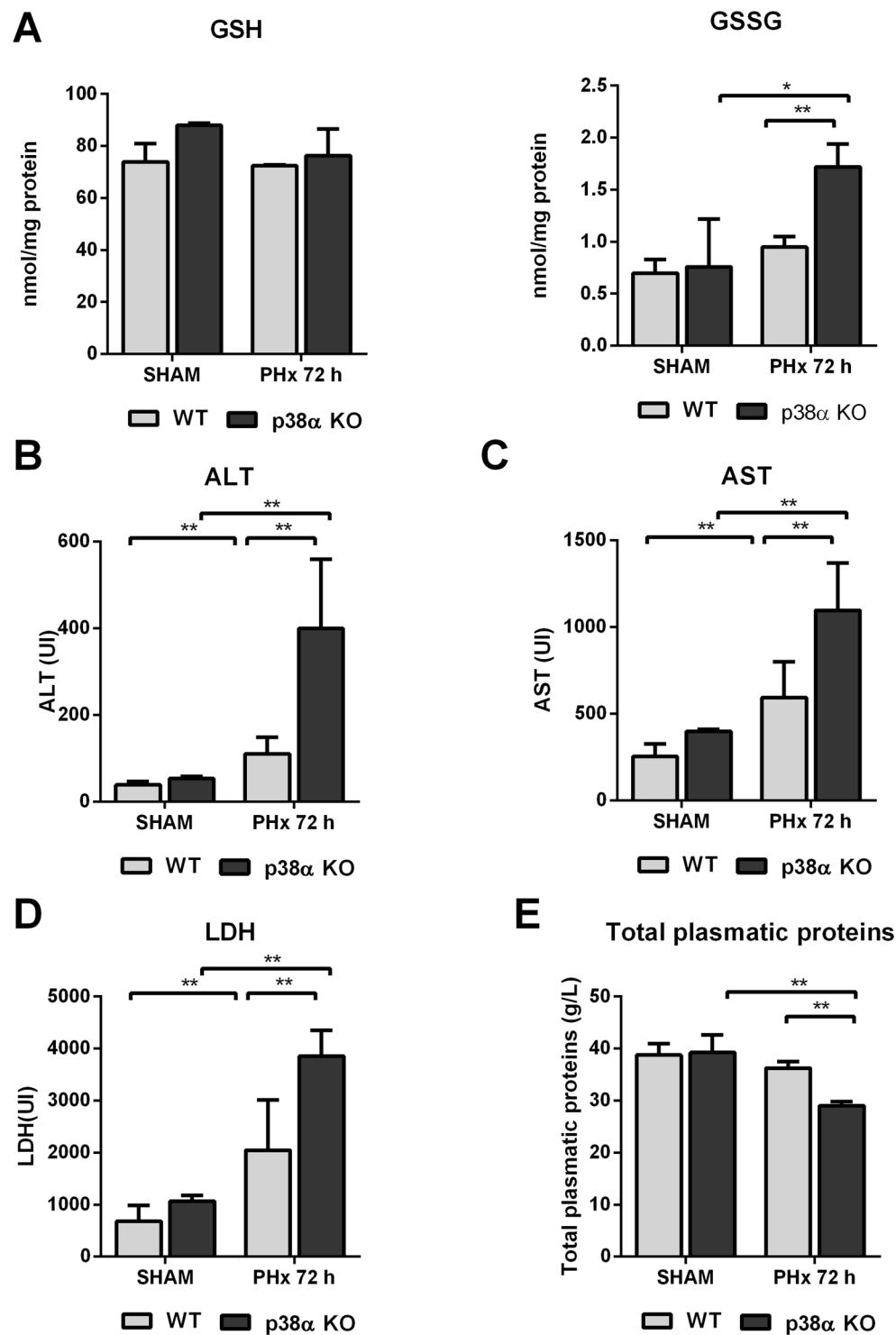


Figure 5. p38 α MAPK deficiency triggers oxidative stress and liver injury after partial hepatectomy. (A) Hepatic levels of reduced (GSH) and oxidized (GSSG) glutathione. (B) Plasma activities of alanine aminotransferase (ALT), (C) aspartate aminotransferase (AST) and (D) lactate dehydrogenase and (E) plasma protein levels in wild type and p38 α knockout mouse after partial hepatectomy. Data are shown as mean and SD. *P < 0.05 **P < 0.01. WT wild type mice; KO p38 α knockout mice; PHx partial hepatectomy.

temperature (23 ± 1 °C), relative humidity (50–60%) and light/dark cycles (12h/12h) with food and water *ad libitum*. The study was approved by the Ethics Committee of Animal Experimentation and Welfare of the University of Valencia (Valencia, Spain).

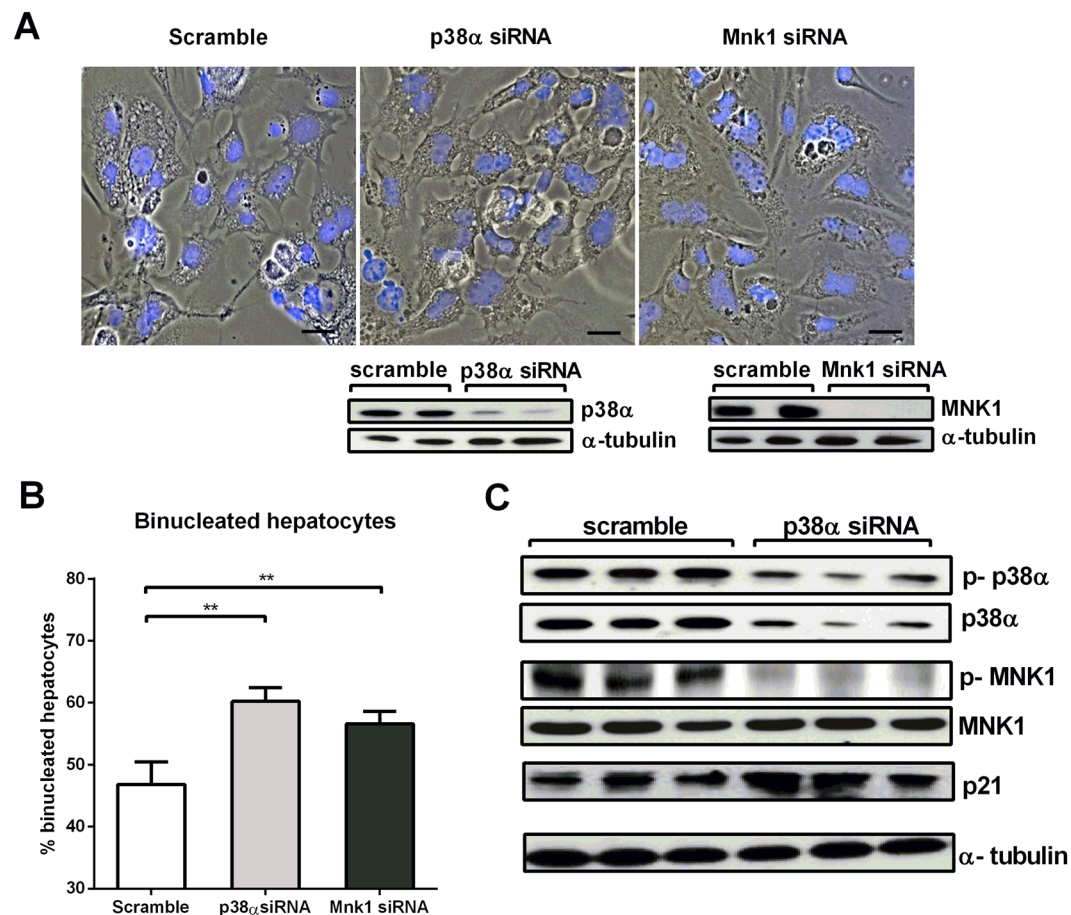


Figure 6. p38 α MAPK silencing in primary hepatocytes increases binucleation through blockade of MNK1 phosphorylation. (A) Representative images of isolated hepatocytes treated with scramble, p38 α MAPK siRNA and Mnk1 siRNA (scale bars = 50 μ m). Control for p38 α MAPK and Mnk1 silencing by siRNA in isolated hepatocytes is also shown. (B) Quantification of the binucleation rate (%) (binucleated hepatocytes/total hepatocytes) in scramble-treated, p38 α MAPK siRNA-treated and Mnk1 siRNA-treated primary culture hepatocytes. At least 20 fields per condition were examined. Data are shown as mean and SD. ** $P < 0.01$. (C) Western blot of isolated hepatocytes scramble-treated, p38 α MAPK siRNA-treated and Mnk1 siRNA-treated for p-p38, p38 α , p-MNK1, MNK1 and p21. α -tubulin was used as loading control. The number of samples per group was 4 to 8.

Partial hepatectomy. Animals were distributed into eight groups: six groups that underwent partial hepatectomy (PHx wild type and PHx p38 α knockout sacrificed at 24, 72 hours or 1 week after PHx), and two groups that were SHAM-operated (SHAM wild type and SHAM p38 α knockout). The total number of mice used was 45: 30 animals underwent partial hepatectomy (15 wild type and 15 p38 α knockout mice sacrificed after PHx) and 15 sham-operated mice (8 wild type and 7 p38 α knockout).

The hepatectomy (PHx) performed in these mice consisted in the resection of 70% of the total liver mass³⁵. The mice were operated under anesthesia (3% isoflurane in oxygen) and with the use of a heating mantle at 37 °C. The animal's abdomen was shaved and disinfected (70% EtOH) to maintain a semi-sterile condition, necessary to reduce the risk of post-operative infections. An incision about 2 cm was made in the abdomen longitudinally along the alba line. Liver sections resected were: right anterior segment, left anterior segment, left posterior segment and omental segment. After suture, the animal was disinfected with iodine tincture and placed on an electric blanket at 37 °C. Both SHAM and PHx animals were treated with analgesia during the entire post-operative period of time (Buprex[®]). Finally, animals were euthanized under anesthesia at 72 hours post-surgery. Blood was extracted and centrifuged 15 min, 1700 rpm at room temperature to obtain plasma samples, which were frozen at -80 °C till analysis.

Culture of primary hepatocytes. Primary mouse hepatocytes were isolated from non-fasting male C57BL/6 mice (3–4 months) by a two-step collagenase perfusion as previously described³⁶. Briefly, cells were seeded on collagen-coated 12-well plate (Corning, Inc.) and cultured at density of 350,000 cells/well in 1 ml medium containing Dulbecco's modified Eagle's medium and Ham's F-12 medium (1:1) supplemented with 10% FBS, 2 mM glutamine, 100 units/ml penicillin, 100 μ g/ml streptomycin, and 1 mM sodium pyruvate (attachment medium) and maintained under a humidity conditions in 95% air and 5% CO₂ at 37 °C for 24 h before siRNA transfection. For cell staining experiments, collaged-coated coverslips were used.

Oligo name	Sequence 5' to 3'
mm.CyclinA1.F	GTCAACCCCGAAAACTGGC
mm.CyclinA1.R	GAGCAACCCGTCGAGTCTT
mm.CyclinB1.F	GCCTGAACCTGAACTTGAACA
mm.CyclinB1.R	ACATCCAGATGTTTCCATCG
mm.CyclinB2.F	ACCCACAGCCTCTGTGAAAC
mm.CyclinB2.R	CTGCAGAGCAGAGCATCAG
mm. CyclinCdc25b.F	AGGGAGAGAAGGTGTCTTACCA
mm. CyclinCdc25b.R	GCCCTTTCGACAGGAGTCAA
mm.CyclinD1.F	ACTGCCGAGAAGTTGTGCAT
mm.CyclinD1.R	AAGCAGTTCCATTTCGAGCAG

Table 1. Primer sequences.

Gene knockdown by siRNA. Cells were transfected with 25 nM siRNAs or with a scrambled siRNA, used as control, following DharmaFECT General Transfection Protocol (Dharmacon) to knockdown mouse p38 α MAPK and Mnk1 expression. Cells were used 48 h later for experiments. *DharmaFECT siRNA Transfection Reagent*, p38 α MAPK siRNA (5 nmol SMARTpool: ON-TARGETplus Mapk14 siRNA L-040125-00-0005), Mnk1 siRNA (5 nmol SMARTpool: ON-TARGETplus Mouse Mknk1 siRNA L-040139-00-0005) and scramble siRNA were obtained from Dharmacon.

Western blotting. For total liver homogenates, protein was extracted with Heidolph (RZR 2021) homogenizer in Hepes lysis buffer pH 7.4 with 1 mM DTT, 1 mM sodium ortovanadate, 50 mM sodium fluoride, 30 mM sodium pyrophosphate, 1% Igepal, 10% glycerol and protease inhibitor cocktail (Sigma Aldrich). To obtain total cell lysates, attached cells were scraped off and incubated for 10 min on ice with lysis buffer. Homogenates and cell lysates were centrifuged during 15 min at 15000 rpm, 4 °C. In case of nuclei isolation, a slight modification of the nuclei isolation method described by³⁷ was used. Chemiluminescence was detected with a charge-coupled device camera (Biorad ChemiDoc XRS+ Molecular Imager and LAS-3000, Fujifilm) using the ECL system (Luminata Classico, Millipore).

Antibodies used were: α tubulin (Sigma Aldrich T6074), p21 (sc-6246), p38 α MAPK (sc-535) from Santa Cruz Biotechnology; H3 (4499), MNK1 (2195), PCNA (2586), p53 (9282), p-H3 (Ser10) (9710), p-MNK1(Thr197/202) (2111), p-p38 (Thr 180/Tyr188) (4511XP) from Cell Signaling Technology. All of them were dissolved in 1% Bovine Serum Albumin (Sigma) in TBS-0.01% Tween 20. The blocking agent was a solution of 5% Bovine Serum Albumin in TBS-0.01% Tween 20.

Secondary antibodies were from Jackson Immunoresearch: Donkey anti rabbit (711-035-152) and donkey anti mouse (715-035-151). They were prepared at 1/40,000 dilution in 1% TBS-0.01% Tween 20.

Real time RT-PCR. A small piece (approximately 30 mg) of liver was homogenized in trizol reagent, and total RNA was isolated by the chloroform:phenol method (Sigma-Aldrich). RT was performed using the Revert Aid kit (Thermo Scientific, Logan, UT). Quantitative PCR experiments were performed on a thermal cycler (I-Cycler + IQ Multicolor Real Time OCR Detection System, Biorad) by using SYBR Green PCR Master Mix (Takara, Otsu, Shiga). Results were normalized using Tbp as reference (mm.tbp.F: CAGCCTTCCACCTTATGCTC; mm.tbp.R: CCGTAAGGCATCATTGGACT). The threshold cycle (Ct) was determined, and relative gene expression levels were subsequently calculated by the $2^{(-\Delta\Delta Ct)}$ formula. Primer sequences used for cyclin expression are shown in Table 1.

Mass spectrometry. Frozen liver samples were homogenized in phosphate saline buffer (PBS) with 10 mM N-ethyl maleimide (NEM). Perchloric acid (PCA) was then added to obtain a concentration of 4% and centrifuged at 15,000 g for 15 min at 4 °C. The concentrations of GSH and GSSG were determined in the supernatants by high-performance liquid chromatography coupled to tandem mass spectrometry (HPLC-MS/MS). The chromatographic system consisted of a Micromass QuatroTM triplequadrupole mass spectrometer (Micromass, Manchester, UK) equipped with a Zspray electrospray ionization source operating in the positive ion mode with a LC-10A Shimadzu (Shimadzu, Kyoto, Japan) coupled to the MassLynx software 4.1 for data acquisition and processing. Samples were analyzed by reverse-phase HPLC with a C18 Mediterranean SEA column (Teknokroma, Barcelona, Spain). The mobile phase consisted of the following gradient system (min/%A/%B) (A, 0.5% formic acid; B, isopropanol/acetonitrile 50/50; 0.5% formic acid): 5/100/0, 10/0/100, 15/0/100, 15.10/100/0, and 60/100/0. The flow rate was set at 0.2 ml/min. Positive ion electrospray tandem mass spectra were recorded using the following conditions: capillary voltage 3.5 kV, source temperature 120 °C, nebulization and cone gases were set at 500 and 30 L/h, respectively. Argon at 1.5610–3 mbar was used as the collision gas for collision-induced dissociation. An assay based on LC-MS/MS with multiple reaction monitoring was developed using the transitions m/z, cone energy (V), collision energy (eV) and retention time (min) for each compound that represents favorable fragmentation pathways for these protonated molecules (Table 2). Calibration curves were obtained using twelve-point (0.01–100 mmol/l) standards (purchased from Sigma-Aldrich, St Louis, USA) for each compound. The concentrations of metabolites were expressed as nmol/mg of protein.

Analyte	Cone (V)	Collision (eV)	Transition (m/Z)	Retention time (min)
GS-NEM	30	15	433 > 304	4.32
GSSG	30	25	613 > 355	1.46

Table 2. Transitions and retention times for analytes determined by LC–MS/MS.

Immunohistochemistry and cell staining. Formalin-fixed, paraffin embedded sections of liver tissue were deparaffinized using Histo-Clear® (National Diagnostics). As an alternative for xylene and antigen retrieval, tissue sections were autoclaved in citrate buffer pH 6 for staining. Slides were blocked with 5% BSA in PBS. Antibodies used in immunofluorescence were as follows: β -catenin (9562), Mnk1 (Thr197/202) (2111), p-H3 (ser10) (9710) and PCNA (2586) from Cell Signaling Technology and β -tubulin (ab7792) from Abcam. All of them were dissolved in 1% Bovine Serum Albumin (Sigma) in TBS-0.3% Tween 20 and purchased from Cell Signaling Technology. Secondary antibodies were: Alexa Fluor anti rabbit (A-21206) and Alexa Fluor anti mouse (A-11002) from Life Technologies. Nuclei were stained with DAPI (Life Technologies, D1306). For binucleation rate (percentage of binucleated cells/total number of cells) and number of nuclei per field, 50–60 slides from all different animals were blindly scored.

For *in vitro* assays, primary hepatocytes seeded on collagen-coated glass coverslips (10 mm) in 12-well plates were fixed with 4% paraformaldehyde for 6 min, washed with PBS and permeabilized with 0.1% Triton X-100 during 5 min. Nuclei were stained with DAPI (Life Technologies, D1306). An OLYMPUS FV1000MPE confocal microscope was used for image acquisition.

Biochemical assays. Liver injury and function was assessed by alanine aminotransferase (ALT, Spinreact 41280), aspartato aminotransferase (AST, Spinreact 41270), and lactate dehydrogenase (LDH, Spinreact 1001260) activities in plasma. Moreover, total plasmatic proteins (Spinreact 1001290) were determined. Plasma samples were analyzed according to the manufacture instructions.

TUNEL assay. Formalin-fixed, paraffin embedded sections were deparaffinized using xylene and then, anti-ger retrieval was performed by citrate buffer (37 °C, 15 minutes). Nucleotide labelling and detection were performed as described following manufacturer's instructions (*In Situ* Cell Death Detection Kit 11 684 817 910, Roche).

Statistical analysis. Results are given as mean \pm standard deviation (s.d.). Significant differences were assessed by one-way analysis of variance (ANOVA) followed by a Tukey's *post-hoc* test. Differences were considered statistically significant at $p < 0.05$.

References

- Cuadrado, A. & Nebreda, A. R. Mechanisms and functions of p38 MAPK signalling. *Biochem J* **429**, 403–417 (2010).
- Campbell, J. S., Argast, G. M., Yuen, S. Y., Hayes, B. & Fausto, N. Inactivation of p38 MAPK during liver regeneration. *Int J Biochem Cell Biol* **43**, 180–188 (2011).
- Tormos, A. M. *et al.* Liver-specific p38alpha deficiency causes reduced cell growth and cytokinesis failure during chronic biliary cirrhosis in mice. *Hepatology* **57**, 1950–1961 (2013).
- Cuenda, A. & Rousseau, S. p38 MAP-kinases pathway regulation, function and role in human diseases. *Biochim Biophys Acta* **1773**, 1358–1375 (2007).
- Awad, M. M., Enslin, H., Boylan, J. M., Davis, R. J. & Gruppiso, P. A. Growth regulation via p38 mitogen-activated protein kinase in developing liver. *J Biol Chem* **275**, 38716–38721 (2000).
- Wagner, E. F. & Nebreda, A. R. Signal integration by JNK and p38 MAPK pathways in cancer development. *Nat Rev Cancer* **9**, 537–549 (2009).
- Thornton, T. M. & Rincon, M. Non-classical p38 map kinase functions: cell cycle checkpoints and survival. *Int J Biol Sci* **5**, 44–51 (2009).
- Hui, L., Bakiri, L., Stepniak, E. & Wagner, E. F. p38alpha: a suppressor of cell proliferation and tumorigenesis. *Cell Cycle* **6**, 2429–2433 (2007).
- Hui, L. *et al.* p38alpha suppresses normal and cancer cell proliferation by antagonizing the JNK-c-Jun pathway. *Nat Genet* **39**, 741–749 (2007).
- Tormos, A. M. *et al.* p38alpha regulates actin cytoskeleton and cytokinesis in hepatocytes during development and aging. *PLoS One* **12**, e0171738 (2017).
- Duncan, A. W. *et al.* The ploidy conveyor of mature hepatocytes as a source of genetic variation. *Nature* **467**, 707–710 (2010).
- Mossin, L., Blankson, H., Huitfeldt, H. & Seglen, P. O. Ploidy-dependent growth and binucleation in cultured rat hepatocytes. *Exp Cell Res* **214**, 551–560 (1994).
- Lu, P. *et al.* Microarray analysis of gene expression of mouse hepatocytes of different ploidy. *Mamm Genome* **18**, 617–626 (2007).
- Gentric, G., Celton-Morizur, S. & Desdouets, C. Polyploidy and liver proliferation. *Clin Res Hepatol Gastroenterol* **36**, 29–34 (2012).
- Gentric, G., Desdouets, C. & Celton-Morizur, S. Hepatocytes polyploidization and cell cycle control in liver physiopathology. *Int J Hepatol* **2012**, 282430 (2012).
- Gerlyng, P. *et al.* Binucleation and polyploidization patterns in developmental and regenerative rat liver growth. *Cell Prolif* **26**, 557–565 (1993).
- Sigal, S. H. *et al.* Partial hepatectomy-induced polyploidy attenuates hepatocyte replication and activates cell aging events. *Am J Physiol* **276**, G1260–1272 (1999).
- Gentric, G. & Desdouets, C. Polyploidization in liver tissue. *Am J Pathol* **184**, 322–331 (2014).
- Miyaoka, Y. *et al.* Hypertrophy and unconventional cell division of hepatocytes underlie liver regeneration. *Curr Biol* **22**, 1166–1175 (2012).
- Guidotti, J. E. *et al.* Liver cell polyploidization: a pivotal role for binuclear hepatocytes. *J Biol Chem* **278**, 19095–19101 (2003).
- Duncan, A. W. Aneuploidy, polyploidy and ploidy reversal in the liver. *Semin Cell Dev Biol* **24**, 347–356 (2013).
- Zou, Y. *et al.* Four waves of hepatocyte proliferation linked with three waves of hepatic fat accumulation during partial hepatectomy-induced liver regeneration. *PLoS One* **7**, e30675 (2012).

23. Fabrikant, J. I. The kinetics of cellular proliferation in regenerating liver. *J Cell Biol* **36**, 551–565 (1968).
24. Cha, H., Wang, X., Li, H. & Fornace, A. J. Jr. A functional role for p38 MAPK in modulating mitotic transit in the absence of stress. *J Biol Chem* **282**, 22984–22992 (2007).
25. Clouston, A. D. *et al.* Fibrosis correlates with a ductular reaction in hepatitis C: roles of impaired replication, progenitor cells and steatosis. *Hepatology* **41**, 809–818 (2005).
26. d'Adda di Fagagna, F. Living on a break: cellular senescence as a DNA-damage response. *Nat Rev Cancer* **8**, 512–522 (2008).
27. Dash, B. C. & El-Deiry, W. S. Phosphorylation of p21 in G2/M promotes cyclin B-Cdc2 kinase activity. *Mol Cell Biol* **25**, 3364–3387 (2005).
28. Lee, K., Kenny, A. E. & Rieder, C. L. P38 mitogen-activated protein kinase activity is required during mitosis for timely satisfaction of the mitotic checkpoint but not for the fidelity of chromosome segregation. *Mol Biol Cell* **21**, 2150–2160 (2010).
29. Rannou, Y. *et al.* MNK1 kinase activity is required for abscission. *J Cell Sci* **125**, 2844–2852 (2012).
30. Gromley, A. *et al.* Centriolin anchoring of exocyst and SNARE complexes at the midbody is required for secretory-vesicle-mediated abscission. *Cell* **123**, 75–87 (2005).
31. Reiling, J. H., Doepfner, K. T., Hafen, E. & Stocker, H. Diet-dependent effects of the Drosophila Mnk1/Mnk2 homolog Lk6 on growth via eIF4E. *Curr Biol* **15**, 24–30 (2005).
32. Kidd, D. & Raff, J. W. LK6, a short lived protein kinase in Drosophila that can associate with microtubules and centrosomes. *J Cell Sci* **110**(Pt 2), 209–219 (1997).
33. Tormos, A. M., Talens-Visconti, R., Nebreda, A. R. & Sastre, J. p38 MAPK: a dual role in hepatocyte proliferation through reactive oxygen species. *Free Radic Res* **47**, 905–916 (2013).
34. Ventura, J. J. *et al.* p38alpha MAP kinase is essential in lung stem and progenitor cell proliferation and differentiation. *Nat Genet* **39**, 750–758 (2007).
35. Higgins, G. M. & Anderson, R. M. Experimental pathology of liver. I. Restoration of liver of the white rat following partial surgical removal. *Arch Pathol* **12**, 186–202 (1931).
36. Benveniste, R., Danoff, T. M., Ilekis, J. & Craig, H. R. Epidermal growth factor receptor numbers in male and female mouse primary hepatocyte cultures. *Cell Biochem Funct* **6**, 231–235 (1988).
37. Graham, J. M. Isolation of nuclei and nuclear membranes from animal tissues. *Curr Protoc Cell Bio* **1** Chapter 3, Unit3 10 (2001).

Acknowledgements

A.M.T. was recipient of a fellowship from the Ministry of Economy and Competitiveness. This work was supported by Grants SAF 2015-71208-R with FEDER funds and CSD-2007-00020 from the Spanish Ministry of Economy and Competitiveness (MINECO, Spain, <http://www.mineco.gob.es/portal/site/mineco/>) and GV PROMETEO II 2014-056 from Generalitat Valenciana to J.S. and R.T.V., and by Grant SAF 2015- 65267-R (MINECO/FEDER) and by Centro de Investigación Biomédica en Red de Diabetes y Enfermedades Metabólicas Asociadas (CIBERdem, ISCIII, Spain) to A.M.V.

Author Contributions

A.M.T., S.R.P. and I.F. did the genotyping of the mice. A.M.T., S.R.P. and R.T.V. performed partial hepatectomy. P.R. isolated hepatocytes and S.R.P. did the *in vitro* experiments. S.R.P., A.M.T. and S.P. carried out all the assays. A.M.T. and S.R.P. performed statistical analysis of the data. R.T.V. and J.S. design the study, supervised the experiments and wrote the manuscript. A.M.V. supervised the *in vitro* experiments and A.M.V. and A.R.N. provided important intellectual input and reviewed the manuscript.

Additional Information

Supplementary information accompanies this paper at <https://doi.org/10.1038/s41598-019-39428-3>.

Competing Interests: The authors declare no competing interests.

Publisher's note: Springer Nature remains neutral with regard to jurisdictional claims in published maps and institutional affiliations.



Open Access This article is licensed under a Creative Commons Attribution 4.0 International License, which permits use, sharing, adaptation, distribution and reproduction in any medium or format, as long as you give appropriate credit to the original author(s) and the source, provide a link to the Creative Commons license, and indicate if changes were made. The images or other third party material in this article are included in the article's Creative Commons license, unless indicated otherwise in a credit line to the material. If material is not included in the article's Creative Commons license and your intended use is not permitted by statutory regulation or exceeds the permitted use, you will need to obtain permission directly from the copyright holder. To view a copy of this license, visit <http://creativecommons.org/licenses/by/4.0/>.

© The Author(s) 2019